Available online at www.sciencedirect.com
ScienceDirect
Trans. Nonferrous Met. Soc. China 28(2018) 2173−2180
Transactions of Nonferrous Metals Society of China
www.tnmsc.cn

Effects of nano-SiC_p content on microstructure and mechanical properties of SiC_p/A356 composites assisted with ultrasonic treatment

Kun HU, Du YUAN, Shu-lin LÜ, Shu-sen WU

State Key Laboratory of Materials Processing and Die & Mould Technology, Huazhong University of Science and Technology, Wuhan 430074, China

Received 19 September 2017; accepted 28 March 2018

Abstract: nano-SiC_p/A356 composites with different nano-SiC_p contents were prepared by squeeze casting after ultrasonic treatment (UT). The effects of SiC_p content on the microstructure and mechanical properties of the nanocomposites were investigated. The results show that with the addition of nano-SiC_p, the microstructure of nanocomposites is obviously refined, the morphology of the α(Al) grains transforms from coarse dendrites to rosette crystals, and long acicular eutectic Si phases are shortened and rounded. The mechanical properties of 0.5%, 1% and 2% (mass fraction) SiC_p/A356 nanocomposites are improved continuously with the increase of nano-SiC_p content. Especially, when the SiC_p content is 2%, the tensile strength, yield strength and elongation are 259 MPa, 144 MPa and 5.3%, which are increased by 19%, 69% and 15%, respectively, compared with those of the matrix alloy. The improvement of strength is attributed to mechanisms of Hall−Petch strengthening and Orowan strengthening.
Key words: nano-SiC_p; aluminum matrix composites; ultrasonic treatment; microstructure; mechanical properties

1 Introduction

Aluminum matrix composites (AMCs) exhibit high specific strength and stiffness, high thermal conductivity, low density, and good corrosion resistance, which offer excellent potential as advanced structural materials in aerospace, electronics, automotive and other fields [1,2]. The main factors affecting the properties of AMCs include reinforcement size, preparation process and mass fraction of the reinforcements [3−6]. Previous studies were mainly focused on the micron-scale particles reinforced AMCs. Although the addition of micron-scale particles in aluminum alloy can improve the strength, the composites cannot be widely applied due to considerable decrease of ductility [7]. In recent years, it has been reported that when the size of the reinforcement is reduced to nano-size (less than 100 nm), the strength of AMCs could be enhanced greatly, while the ductility could be maintained or even increased [8−10].

Currently, there are several fabrication methods of AMCs, such as powder metallurgy [11,12], spray deposition, infiltration method and stir casting [13,14]. Stir casting has the advantages of low cost, simple process, near net shaping, and little limitation for the size and shape of the parts compared with other techniques [15]. Since nanoparticles, having high specific surface area, are easy to agglomerate spontaneously, it is difficult to disperse them uniformly by conventional stir casting in aluminum melt [16]. Ultrasonic treatment (UT) is a promising way to treat the molten aluminum alloys and has been extensively used in purifying, degassing [17], and refining microstructure of the alloys [18,19]. YANG et al [20] stated that UT was also an effective means of dispersing nanoparticles due to ultrasonic cavitation and acoustic streaming effects when introducing the ultrasonic energy into melt. Ultrasonic cavitation in the aluminum melt can produce transient micro “hot spots” with very high pressure and temperature, which can effectively break up the nanoclusters and improve the wettability of the ceramic particles in aluminum melt [21]. Meanwhile, acoustic streaming can accelerate the movement and uniform distribution of nanoparticles in the melt. In a word, UT is an impactful means for preparing nanocomposites.

So far, a lot of research has been carried out about the effects of the content of micron-scale reinforcements on the microstructure and mechanical properties of metal

Foundation item: Project (51574129) supported by the National Natural Science Foundation of China; Project (2016209A001) supported by JCKY Foundation, China
Corresponding author: Shu-sen WU; Tel:+86-27-87556262; E-mail: ssw636@hust.edu.cn
DOI: 10.1016/S1003-6326(18)64862-9

matrix composites [22]. MA et al [23] stated that the increase of volume fraction of SiC_p (5−15 μm) led to size reduction of eutectic Si and also changed its morphology in Al−20Si alloy. RAHMANA and AL RASHED [24] reported that the wear resistance of AMCs showed an improvement with increasing content of SiC_p (53−74 μm), and 20% (mass fraction) SiC_p reinforced AMC showed maximum wear resistance, hardness and tensile strength. However, relevant studies about the influence of different contents of nanoparticles are still limited [25,26]. Nanoparticles have more unique properties, for example, they can help increasing strength by obstructing dislocation and grain boundary motion more than micron particles, and strengthening mechanisms of these two kinds of particles on the matrix alloy are different [8]. In this work, the effect of different contents of nano-SiC_p on α(Al) and eutectic Si is studied by means of microstructure analysis and mechanical properties test, and corresponding refinement mechanism is also discussed.

2 Experimental

Figure 1 showed SE image of the as-received nano-SiC_p and the average size was 40 nm. Hypoeutectic Al−Si alloy A356 was selected as the matrix material considering that at least 7% (mass fraction) of Si can effectively inhibit the interfacial reaction when the temperature of aluminum melt is up to 700 °C [27]. Before preparing nanocomposites, nano-SiC_p was firstly oxidized for 2 h at 1000 °C to ensure the formation of SiO_2 layer on the surface of SiC_p for the purpose of preventing harmful reaction with Al melt [5]. Then, nanoparticles were milled with pure Al powders (70 μm) by high energy ball milling to produce nearly spherical composite granules with diameters of 0.8−2 mm in order to achieve the pre-dispersion of nano-SiC_p in Al powders and clear the air attached to the nano-SiC_p surface [13]. The ball milling process adopted the intermittent mode of milling for 1 h and resting for 30 min in a cycle, the rotation speed was 300 r/min and time was 14 h.

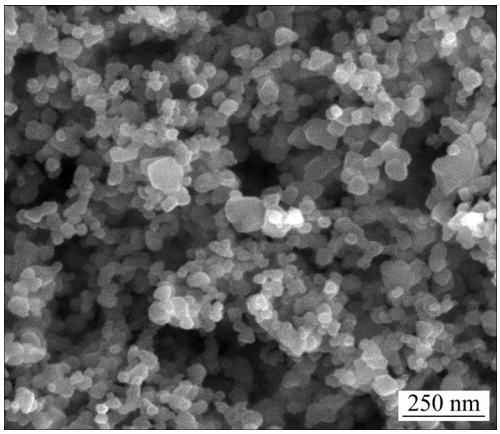

Fig. 1 SE image of as-received nano-SiC_p

Commercial pure Al and Al−24.5Si master ingots were charged into electric resistance furnace and melted. A proper constituent of mentioned composite granules was introduced to the melt by mechanical stirring under the condition of argon gas protection when the temperature of melt was 730 °C, and the speed of mechanical stirring was about 180 r/min. After the granules were completely melted, the chemical compositions of the melt reached the compositions of A356 alloy. Then, the melt containing nano-SiC_p was degassed for 10 min with high purity argon gas. About 300 g melt was taken into a preheated sample cup for ultrasonic treatment in the control of the melt temperature at 700 °C. The ultrasonic treatment device consisted of a transducer with a maximum power of 2.8 kW and frequency of 20 kHz. The melt was treated for 3 min and immediately poured into a permanent steel mold preheated to 200 °C, squeeze cast and solidified under pressure of 100 MPa. Then, a round test bar with diameter of 30 mm and length of 100 mm was obtained. The contents of nano-SiC_p in the SiC_p/A356 nanocomposites were 0.5%, 1% and 2% (mass fraction), respectively. In order to make a relevant comparison, A356 alloy without nano-SiC_p addition was also prepared with ultrasonic treatment and cast under the same conditions.

The microstructure was observed with an optical microscope (OM, Axiovert 200MAT), a scanning electron microscope (SEM, JEOL−7600L) and a transmission electron microscopy (TEM, Tecnai G2 F30). Specimens for observation under OM and SEM were cut from the center of the casting and then ground, polished and etched by 0.5% HF solution. The average secondary dendrite arm spacing (SDAS) of primary α(Al) dendrites in nanocomposites with different SiC_p contents was measured from more than 10 optical micrographs by Imagine Pro Plus Software. Specimens for TEM examination were ground to 50 μm in thickness firstly and then thinned by ion beam to about 5 μm. The room temperature tensile test was conducted on a Shimadzu AG IC−100 kN testing instrument at a drawing speed of 1 mm/min and corresponding samples were machined according to ASTM specification B557M−84. Tensile data were taken from the average value of three specimens.

3 Results and discussion

3.1 Effects of nano-SiC_p content on microstructure

Figure 2 shows the optical micrographs of the as-cast A356 alloy and its nanocomposites with different contents of nano-SiC_p. Figure 3 reveals the average SDAS

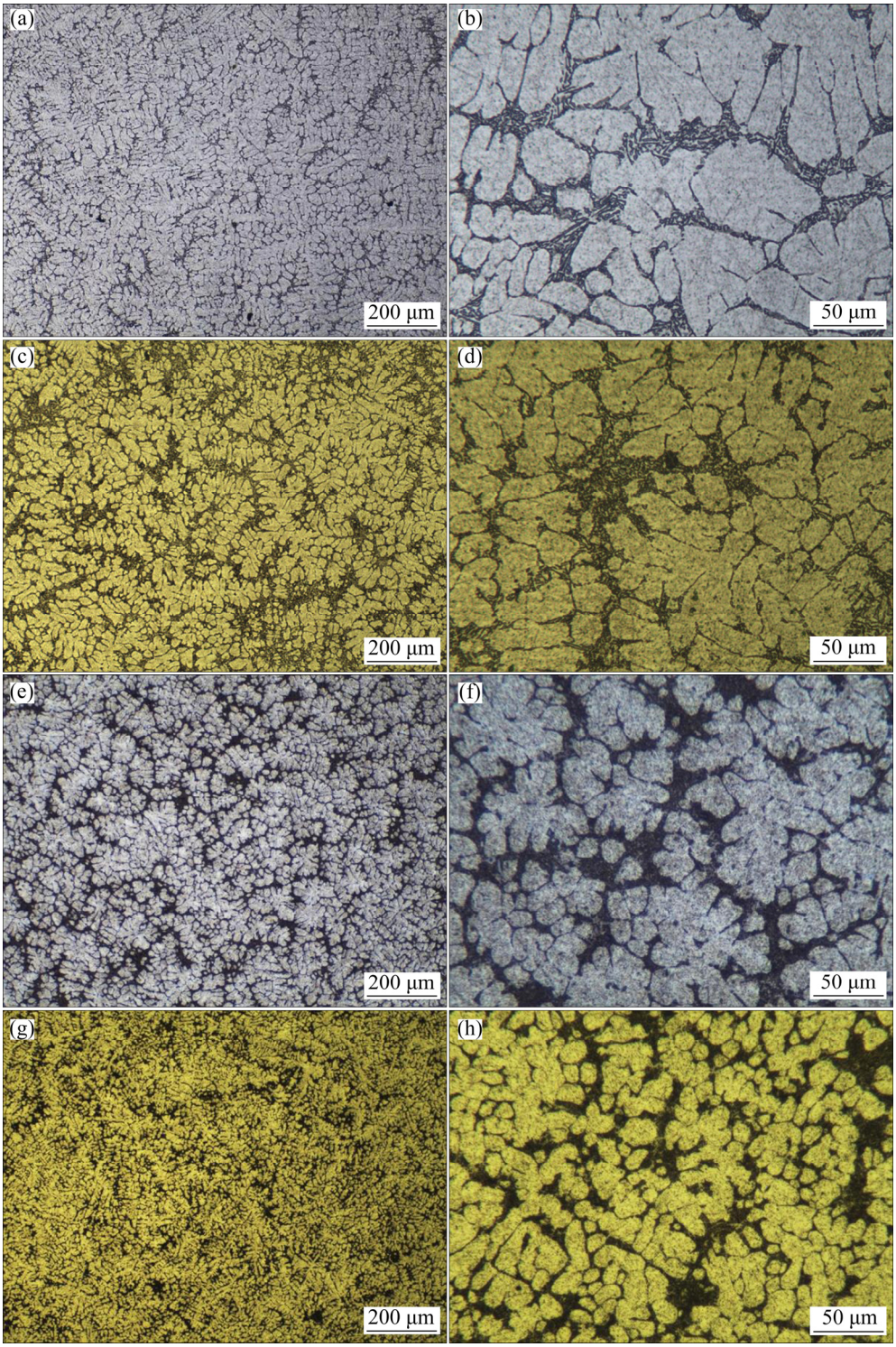

Fig. 2 Optical micrographs of A356 and its nanocomposites with different nano-SiC_p contents: (a, b) Matrix alloy A356; (c, d) 0.5% SiC_p/A356; (e, f) 1% SiC_p/A356; (g, h) 2% SiC_p/A356

values of A356 alloy and SiC_p/A356 nanocomposites. It can be seen that the addition of SiC_p has a great impact on the morphology and grain size of the primary α(Al) of A356 alloy and its nanocomposites. As shown in Figs. 2(a) and (b), the microstructure of A356 is composed of coarse primary α(Al) dendrites and long acicular eutectic Si which is unevenly distributed in the alloy. After the addition of 0.5% (mass fraction) SiC_p to matrix alloy, the dendrite length of the α(Al) is declined from 220 to 160 μm, and the average SDAS values are decreased by 13.7% from 15.3 to 13.2 μm, as indicated in Fig. 3. When the content of SiC_p increases further to 1% and 2% (mass fraction), the average SDAS values of α(Al) are 11.3 and 8.9 μm, decreased by 26.1%

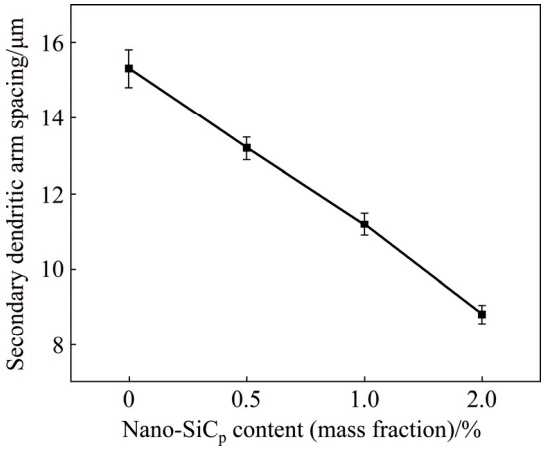

Fig. 3 Secondary dendritic arm spacing (SDAS) of α(Al) in nanocomposites with different nano-SiC_p contents

and 41.8%, respectively. Besides, the morphology of α(Al) dendrites evolves into rosette crystals or equiaxed grains (Figs. 2(e)−(h)). Moreover, it can be seen from Figs. 2(b) and (d) that when the SiC_p content is 0.5%, the long acicular eutectic Si is also refined, and its length decreases as compared with that of the matrix alloy. Therefore, images under higher magnification which can confirm the refinement of eutectic Si in nanocomposites with different nano-SiC_p contents are needed.

The effect of different contents of nano-SiC_p on the eutectic Si can be more evidently seen in SE images (Fig. 4). As shown in Fig. 4(a), eutectic Si exhibits the shape of long plate whose length is up to 5 μm in A356 matrix alloy. When 0.5% SiC_p is added to the matrix alloy, it can be obviously observed that the morphology of eutectic Si has changed greatly (Fig. 4(b)). The long acicular eutectic Si turns into short plate partly with its length decreased and its width increased. Moreover, with the increase of SiC_p content, the length and width of eutectic Si decrease simultaneously, and the morphology tends to be rounder (Figs. 4(c) and (d)) compared with that of the matrix alloy. This suggests that the addition of nano-SiC_p can refine eutectic Si in A356 alloy.

According to the above microstructure observation, a model describing microstructure evolution of nano-SiC_p/A356 composite melt can be proposed (Fig. 5) before the eutectic reaction takes place. SiC_p are uniformly distributed in molten aluminum after ultrasonic treatment (Fig. 5(a)). When the temperature of the composite melt drops to near the liquidus temperature, primary α(Al) grains nucleate and grow (Fig. 5(b)). Meanwhile, nano-SiC particles are pushed by the solidification front, and then gather along the solid−liquid interface, which will inhibit the growth of primary α(Al) (Fig. 5(c)). With the increase of nano-SiC_p content, the restriction of SiC_p on the growth of α(Al) is more obvious, as shown in Fig. 3. The addition of SiC_p can not only refine the primary α(Al), but also have a significant impact on the morphology and size of eutectic Si. During the solidification of nanocomposites, most of SiC_p would concentrate in the residual liquid phase due

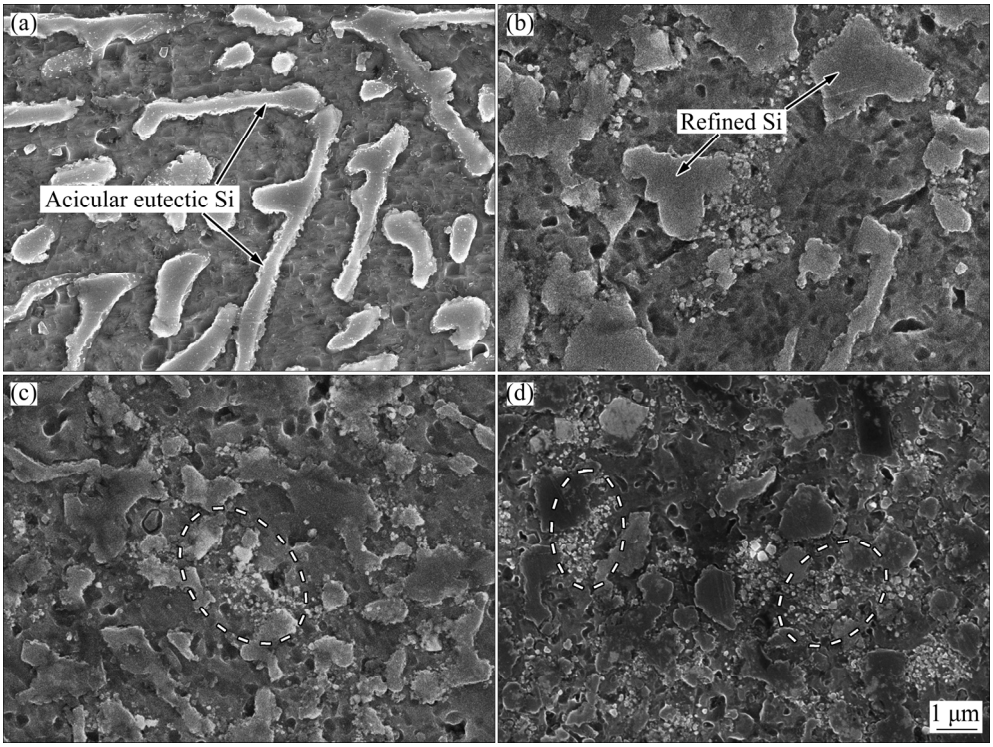

Fig. 4 SE images of A356 and its nanocomposites with different nano-SiC_p contents: (a) Matrix alloy A356; (b) 0.5% SiC_p/A356; (c) 1% SiC_p/A356; (d) 2% SiC_p/A356

to the pushing by the interface. The growing space of eutectic Si is occupied by SiC_p which are apt to distribute on the edge of Si phase (white circles as indicated in Figs. 4(c) and (d)) when the temperature of melt is below eutectic point. It can be inferred that the refinement of eutectic Si is related to inhibition effect of SiC_p. Another refinement reason may be that some nano-SiC_p, after the amorphous SiO_2 layer on its surface is consumed, can act as the heterogeneous core of eutectic Si [28], thus increasing the amount of nucleation agent and refining the eutectic Si. However, the refinement of eutectic Si is not homogeneous, as shown in Figs. 4(c) and (d). When nano-SiC particles are pushed by the primary α(Al) and then agglomerate together in the eutectic region, SiC_p would not reach the optimum extent to impede the growth of Si phase in some regions [29].

Figure 6 shows TEM micrograph and electron diffraction pattern of nano-SiC_p. The reinforcement used in this experiment is β-SiC which has a cubic structure, and the lattice parameters are $a=b=c=0.434$ nm. According to the electron diffraction pattern (Fig. 6(b)), $d_A=0.1306$ nm, $d_B=0.1210$ nm, $d_C=0.2954$ nm, $\theta_{AB}=23.16°$ and $\theta_{BC}=66.19°$. These parameters can match the $d_{(311)}$, $d_{(320)}$, $d_{(01\bar{1})}$, $\theta_{(311)//(320)}$ and $\theta_{(320)//(01\bar{1})}$ in the β-SiC crystal system. The electron diffraction pattern confirms that the nano-particles are SiC_p. As also shown in Fig. 6(a), nano-SiC particles distribute evenly in the aluminum matrix.

3.2 Effects of nano-SiC_p content on mechanical properties

Figure 7 shows the mechanical properties of as-cast A356 and its nanocomposites with different contents of nano-SiC_p. When adding 0.5% SiC_p to the matrix alloy, the ultimate tensile strength (UTS), yield strength (YS) and elongation (EI) are 223 MPa, 93 MPa and 4.7%, only improved by 3%, 9% and 2%, respectively, compared with those of the matrix alloy. However, when the content of SiC_p is increased to 2%, the mechanical properties are greatly improved and the tensile strength and yield strength of the nanocomposites are 259 and 144 MPa, which are increased by 19% and 69%, respectively. Most importantly, the elongation is enhanced by 15%, up to 5.3%, which is higher than what is reported in the Al matrix composite using traditional reinforcements such as micron-sized particles and other

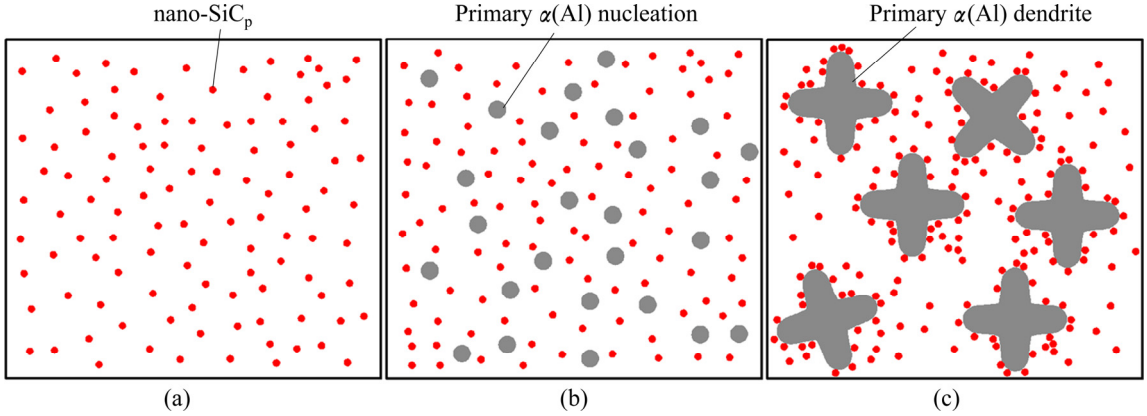

Fig. 5 Schematic diagram of microstructure evolution of nano-SiC_p/A356 composite melt before eutectic reaction: (a) Uniformly distributed nano-SiC_p in composites melt; (b) Nucleation of primary α(Al); (c) Growth of α(Al) grains

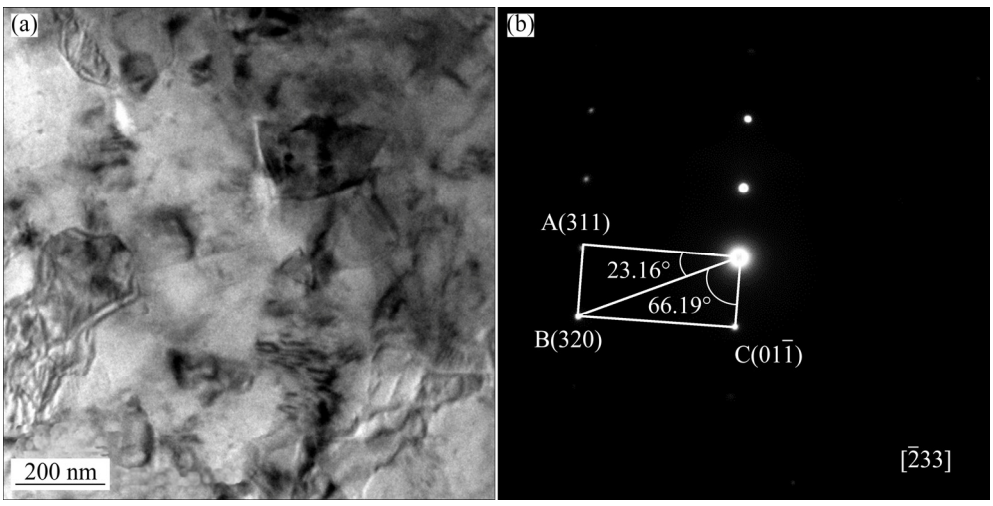

Fig. 6 TEM micrograph (red marks indicating nano-SiC_p) (a) and electron diffraction pattern of SiC_p (b)

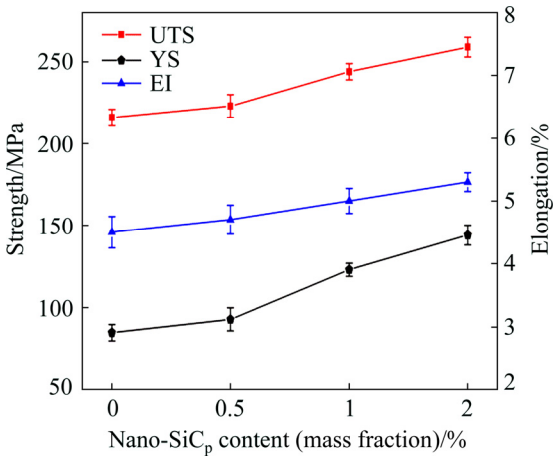

Fig. 7 Mechanical properties of A356 and its nanocomposites

techniques for preparing composites with high volume fraction [7,30].

In this experiment, the enhancement in strength of nanoparticles reinforced metal matrix composites should be attributed to Hall−Petch strengthening and Orowan strengthening. Reduction in grain size increases the yield strength of the nanocomposites according to the Hall−Petch formula: $\sigma_y=\sigma_0+k_y d^{-1/2}$, where σ_0 represents the initial yield strength of the material, k_y is the material constant and d is the grain size of the material. In the nano-SiC_p/A356 composites with different SiC_p contents (Fig. 2), the primary α(Al) grains are clearly refined compared with those in the matrix alloy, which leads to the increase of yield strength of the composite. Meanwhile, it is known that the Orowan strengthening mechanism is significant when the reinforcements are less than 1 μm in size and uniformly distributed in the matrix ally. The average size of SiC_p used in this experiment is about 40 nm, and SiC_p can inhibit the movement of dislocation, which will lead to the increase of the strength of the composites.

The addition of nano-SiC_p in this experiment also improves the elongation of the material, which may be partly due to the refinement of eutectic Si. During tensile process, the non-refined eutectic Si that has sharp tips and edges will produce large stress concentration, which is easy for micro-cracks to nucleate and propagate. Therefore, the alloy will exhibit poor plasticity. With nano-SiC_p addition, the growth of eutectic Si is inhibited and long acicular eutectic Si is shortened and rounded. Thus, the stress concentration is weakened, the crack is difficult to initiate and the elongation is improved. The less content of particles is added, the less refinement effect is obtained. Therefore, when less content (0.5% and 1.0%) is added, the elongation is not obviously changed. With the increase of particle content to 2%, there is a significant enhancement in elongation by 15%.

Figure 8 shows SE images of the tensile fracture surfaces of A356 and 2% SiC_p/A356 nanocomposite. The fracture morphology of A356 presents obviously brittle fracture with the river pattern of the cleavage surface and a few tearing edges in Fig. 8(a). The fracture of A356 starts mainly from the interface between the eutectic Si and the eutectic α(Al) in eutectic region, and then develops into transgranular fracture. However, when adding 2% nano-SiC_p, the eutectic Si and primary α(Al) are refined at the same time. As a result, the nanocomposite has small and uniform fracture surfaces (Fig. 8(b)). The amount of tearing ridge increases, and there are a large number of small quasi-cleavage planes and a few dimples between the tearing ridges, which is beneficial for the improvement in the strength and elongation of composites.

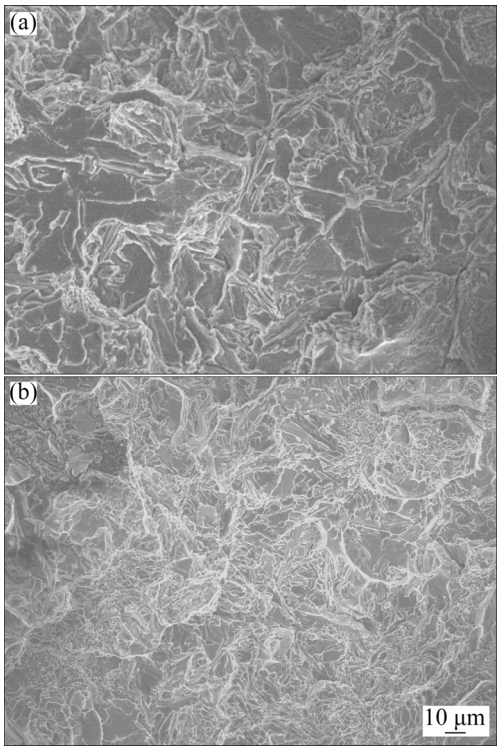

Fig. 8 SE images of fracture surfaces: (a) A356; (b) 2% SiC_p/A356

4 Conclusions

1) The addition of nano-SiC_p has a great influence on the primary α(Al) crystals in SiC_p/A356 nanocomposites. With the increase of nano-SiC_p content, the morphology of α(Al) grains changes from coarse dendrites to rosette crystals and the size of grains is continuously reduced. Especially, when the SiC_p content is 2% (mass fraction), the average SDAS of α(Al) is 8.9 μm, which is reduced by 42% compared with that of the matrix alloy.

2) The addition of nano-SiC_p can also refine eutectic Si phase. The morphology of eutectic Si becomes

gradually shorter and rounder when the content of SiC_p is increased.

3) With the increase of nano-SiC_p content, the mechanical properties of the composite materials are greatly improved. When the content of nano-SiC_p is 2% (mass fraction), the tensile strength, yield strength and elongation are 259 MPa, 144 MPa and 5.3%, which are increased by 19%, 69% and 15%, respectively, compared with those of the A356 matrix alloy.

References

[1] PRAMANIK A. Effects of reinforcement on wear resistance of aluminum matrix composites [J]. Transaction of Nonferrous Metals Society of China, 2016, 26: 348−358.

[2] KNOWLES A J, JIANG X, GALANO M, AUDEBERT F. Microstructure and mechanical properties of 6061 Al alloy based composites with SiC nanoparticles [J]. Journal of Alloys and Compounds, 2014, 615(1): s401−s405.

[3] DEHNAVI M R, NIROUMAND B, ASHRAFIZADEH F, ROHATGI P K. Effects of continuous and discontinuous ultrasonic treatments on mechanical properties and microstructural characteristics of cast Al413−SiC_{np} nanocomposite [J]. Materials Science and Engineering A, 2014, 617(1): 73−83.

[4] SU H, GAO W L, ZHANG H, LIU H B, LU J, LU Z. Study on preparation of large sized nanoparticle reinforced aluminum matrix composite by solid-liquid mixed casting process [J]. Materials Science and Technology, 2012, 28(2): 178−183.

[5] ZHANG Hong-wei, GENG Lin, GUAN Li-na, HUANG Lu-jun. Effects of SiC particle pretreatment and stirring parameters on the microstructure and mechanical properties of SiC_p/Al−6.8Mg composites fabricated by semi-solid stirring technique [J]. Materials Science and Engineering A, 2010, 528(1): 513−518.

[6] TAHAMTAN S, EMAMY M, HALVAEE A. Effects of reinforcing particle size and interface bonding strength on tensile properties and fracture behavior of Al-A206/alumina micro/nanocomposites [J]. Journal of Composite Materials, 2014, 48(27): 3331−3346.

[7] MAZAHERY A, ABDIZADEH H, BAHARVANDI H R. Development of high performance A356/nano−Al_2O_3 composites [J]. Materials Science and Engineering A, 2009, 518(1−2): 61−64.

[8] AKBARI M K, BAHARVANDI H R, SHIRVANIMOGHADDAM K. Tensile and fracture behavior of nano/micro TiB_2 particle reinforced casting A356 aluminum alloy composites [J]. Materials and Design, 2015, 66: 150−161.

[9] MATIN A, SANIEE F F. ABEDI H R. Microstructure and mechanical properties of Mg/SiC and AZ80/SiC nano-composites fabricated through stir casting method [J]. Materials Science and Engineering A, 2015, 625: 81−88.

[10] NGUYEN Q B, GUPTA M. Enhancing compressive response of AZ31B using nano-Al_2O_3 and copper additions [J]. Journal of Alloys and Compounds, 2010, 490(1−2): 382−387.

[11] YING D Y, ZHANG D L. Processing of Cu-Al_2O_3 metal matrix nanocomposite materials by using high energy ball milling [J]. Materials Science and Engineering A, 2000, 286(1): 152−156.

[12] ZHANG Liu, XU Han-qing, WANG Zhi, LI Qing-gang, WU Jun-yan. Mechanical properties and corrosion behavior of Al/SiC composites [J]. Journal of Alloys and Compounds, 2016, 678: 23−30.

[13] AMIRKHANLOU S, NIROUMAND B. Fabrication and characterization of Al356/SiC_p semisolid composites by injecting SiC_p containing composite powders [J]. Journal of Materials Processing Technology, 2012, 212(4): 841−847.

[14] EZATPOUR H R, SAJJADI S A, SABZEVAR M H, HUANG Y Z. Investigation of microstructure and mechanical properties of Al6061-nanocomposite fabricated by stir casting [J]. Materials and Design, 2014, 55(6): 921−928.

[15] HASHIM J, LOONEY L, HASHMI M S J. Metal matrix composites: Production by the stir casting method [J]. Journal of Materials Processing Technology, 1999, 92−93: s1−s7.

[16] LAN J, YANG Y, LI X C. Microstructure and microhardness of SiC nanoparticles reinforced magnesium composites fabricated by ultrasonic method [J]. Materials Science and Engineering A, 2004, 386(1−2): 284−290.

[17] LIU Xuan, ZHANG Cheng, ZHANG Zhi-qiang, XUE Ji-lai, LE Qi-chi. The role of ultrasound in hydrogen removal and microstructure refinement by ultrasonic argon degassing process [J]. Ultrasonics Sonochemistry, 2017, 38: 455−462.

[18] YANG Xiong, WU Shu-sen, LÜ Shu-lin, HAO Liang-yan, FANG Xiang-gang. Refinement of LPSO structure in Mg-Ni-Y alloys by ultrasonic treatment [J]. Ultrasonics Sonochemistry, 2018, 40: 472−479.

[19] LIN Chong, WU Shu-sen, ZHONG Gu, WAN Li, AN Ping. Effect of ultrasonic vibration on Fe-containing intermetallic compounds of hypereutectic Al−Si alloys with high Fe content [J]. Transaction of Nonferrous Metals Society of China, 2013, 23: 1245−1252.

[20] YANG Y, LAN J, LI X C. Study on bulk aluminum matrix nano-composite fabricated by ultrasonic dispersion of nano-sized SiC particles in molten aluminum alloy [J]. Materials Science and Engineering A, 2004, 380(1): 378−383.

[21] ESKIN G I, ESKIN D G. Production of natural and synthesized aluminum-based composite materials with the aid of ultrasonic (cavitation) treatment of the melt [J]. Ultrasonics Sonochemistry, 2003, 10: 297−301.

[22] PERUMAL A, SHYNI P C. SiC content effect on the properties of Cu−SiC composites produced by mechanical alloying [J]. Journal of Alloys and Compounds, 2015, 632: 707−710.

[23] MA P, ZOU C M, WANG H W, SCUDINO S, FU B G, WEI Z J, KÜHN U, ECKERT J. Effects of high pressure and SiC content on microstructure and precipitation kinetics of Al-20Si alloy [J]. Journal of Alloys and Compounds, 2014, 586(4): 639−644.

[24] RAHMANA M H, AL RASHED M H H. Characterization of silicon carbide reinforced aluminum matrix composites [J]. Procedia Engineering, 2014, 90: 103−109.

[25] JIANG Ju-fu, WANG Ying. Microstructure and mechanical properties of the semisolid slurries and rheoformed component of nano-sized SiC/7075 aluminum matrix composite prepared by ultrasonic-assisted semisolid stirring [J]. Materials Science and Engineering A, 2015, 639: 350−358.

[26] KANDEMIR S. Microstructure and mechanical properties of A357/SiC nanocomposites fabricated by ultrasonic cavitation-based dispersion of ball-milled nanoparticles [J]. Journal of Composite Materials, 2016, 51: 395−404.

[27] LEE J C, BYUN J Y, PARK S B, LEE H I. Prediction of Si contents to suppress the formation of Al_4C_3 in the SiC_p/Al Composites [J]. Acta Materialia, 1998, 46(8): 2635−2643.

[28] ZHANG Q, XIU Z Y, SONG M H, WU G H. Microstructure and properties of a 70vol.% SiC_p/Al−12Si composite for electronic packaging [J]. Materials Science Forum, 2005, 475: 881−884.

[29] CHOI H, KONISHI H, LI X C. Al_2O_3 nanoparticles induced simultaneous refinement and modification of primary and eutectic Si particles in hypereutectic Al−20Si alloy [J]. Materials Science and Engineering A, 2012, 541(16): 159−165.

[30] WANG Lei, QIU Feng, ZOU Qian, YANG De-Long. Microstructures and tensile properties of nano-sized SiC_p/Al−Cu composites fabricated by semisolid stirring assisted with hot extrusion [J]. Materials Characterization, 2017, 131:195−200.

纳米 SiC_p 含量对超声方法制备的 SiC_p/A356 复合材料组织和性能的影响

胡 坤，袁 渡，吕书林，吴树森

华中科技大学 材料成形与模具技术国家重点实验室，武汉 430074

摘 要：采用超声处理和挤压铸造制备具有不同纳米 SiC 颗粒含量的复合材料，并研究 SiC_p 含量对纳米复合材料显微组织和力学性能的影响。结果表明，随着纳米颗粒的加入，显微组织明显细化，α(Al)晶粒形貌由粗大枝晶向玫瑰晶转变，长针状共晶硅逐渐变短并且圆整。随着颗粒含量的增加，复合材料的抗拉强度、屈服强度和伸长率均持续增加。特别是，当 SiC 加入量达到 2%(质量分数)时，抗拉强度、屈服强度和伸长率分别为 259 MPa、144 MPa 和 5.3%，与基体合金相比分别增加 19%、69%和 15%。强度的提升是由于 Hall−Petch 强化和 Orowan 强化。

关键词：纳米 SiC_p；铝基复合材料；超声处理；显微组织；力学性能

(Edited by Bing YANG)